

8-6-2013

# Design and Construction of a Nernst Effect Measuring System

Warner E. Sevin

*University of New Orleans*, wsevin@uno.edu

Follow this and additional works at: <http://scholarworks.uno.edu/td>

---

## Recommended Citation

Sevin, Warner E., "Design and Construction of a Nernst Effect Measuring System" (2013). *University of New Orleans Theses and Dissertations*. Paper 1684.

This Thesis is brought to you for free and open access by the Dissertations and Theses at ScholarWorks@UNO. It has been accepted for inclusion in University of New Orleans Theses and Dissertations by an authorized administrator of ScholarWorks@UNO. The author is solely responsible for ensuring compliance with copyright. For more information, please contact [scholarworks@uno.edu](mailto:scholarworks@uno.edu).

# Design and Construction of a Nernst Effect Measuring System

A Thesis

Submitted to the Graduate Faculty of the  
University of New Orleans  
in partial fulfillment of the  
requirements for the degree of

Master of Science  
In  
Applied Physics

By

Warner Earl Sevin

B.S. Loyola University New Orleans, 2011

August 2013

## Table of Contents

<b>List of Figures</b>	<b>iv</b>
<b>List of Tables</b>	<b>v</b>
<b>Abstract</b>	<b>vi</b>
Chapter 1. Introduction.....	1
1.1. Introduction to Thermoelectric Materials .....	1
1.2. Goals.....	1
Chapter 2. Background Theory .....	2
2.1. Overview of Thermoelectric Effects.....	2
2.1.1. Electrical Conductivity .....	2
2.1.2. The Seebeck Effect .....	2
2.1.3. The Peltier Effect .....	3
2.1.4. The Hall Effect.....	4
2.1.5. The Righi-Leduc Effect .....	5
2.1.6. The Nernst Effect.....	6
2.1.7. The Ettingshausen Effect .....	6
Chapter 3. Experimental Setup.....	8
3.1. Equipment .....	8
3.2. Sample Setup.....	10
3.3. LabView Program Design.....	14
3.4. Taking Measurements .....	15
3.5. Approximations for the Nernst Coefficient.....	16
Chapter 4. Results.....	18
Chapter 5. Discussion .....	29
5.1. Improvement of Results .....	29
5.1.1. Error Analysis .....	31
5.1.2. Improvements to Experimental Setup.....	33

Chapter 6. Conclusions.....	34
-----------------------------	----

<b>Bibliography</b>	<b>35</b>
---------------------	-----------

<b>Vita</b>	<b>36</b>
-------------	-----------

## List of Figures

Figure 2.1 A schematic of a simple thermocouple. ....	3
Figure 2.2. A visual summary of the thermomagnetic effects. ....	8
Figure 3.1. Nernst effect measuring system in our lab. ....	9
Figure 3.2. Sample lead diagram .....	10
Figure 3.3. Sample lead photograph .....	11
Figure 3.4. Connection schematic diagram .....	12
Figure 3.5. A sample mounted in the chamber. ....	13
Figure 4.1. Raw data for BiNiTe sample at constant temperature gradient.....	19
Figure 4.2. Plot of C/D Voltage vs. Magnetic Field for BiNiTe sample. ....	20
Figure 4.3. Plot of E/F Voltage vs. Magnetic Field for BiNiTe sample .....	21
Figure 4.4. Raw data for BiNiTe sample at constant magnetic field.....	22
Figure 4.5. Plot of E/F Voltage vs. $\Delta T$ for BiNiTe sample at constant magnetic field. ....	22
Figure 4.6. Plot of C/D Voltage vs. $\Delta T$ for BiNiTe sample at constant magnetic field. ....	23
Figure 4.7. Raw data for BiSbTe sample at constant temperature gradient .....	25
Figure 4.8. Graph of E/F Voltage vs. Magnetic Field for BiSbTe sample. ....	26
Figure 4.9. Graph of C/D Voltage vs. Magnetic Field for BiSbTe sample. ....	27
Figure 4.10. Raw data for BiSbTe sample at constant magnetic field.....	27
Figure 4.11. Plot of E/F Voltage vs. $\Delta T$ for BiSbTe sample. ....	28
Figure 4.12. Plot of C/D Voltage vs. $\Delta T$ for BiSbTe sample. ....	29
Figure 5.1. Misalignment in the voltage leads on the sample.....	30
Figure 5.2. Graph of Temperature vs. Thermocouple EMF. ....	32

## **List of Tables**

Table 2.1 Summary of non-magnetic thermoelectric effects.....	4
Table 2.2. Summary of the thermomagnetic effects. ....	8
Table 5.1. Summary of error terms.....	33

## **Abstract**

An experimental Nernst effect measuring system is designed and constructed. The ability to measure the Nernst effect allows completion of a thermoelectric suite of measurements consisting of electrical conductivity, the Seebeck effect, the Hall effect, and the Nernst effect. This suite of measurements gives information about electron transport, carrier concentration, and electron scattering within a thermoelectric sample. Programs were designed in LabView to control the various instruments in the measuring system. Measurements of the Nernst effect were taken on two thermoelectric samples, bismuth nickel telluride and bismuth antimony telluride. These measurements were taken at both constant temperature and constant magnetic field. An error analysis of the Nernst effect measuring system is also presented, with consideration as to future work that can be done to improve the quality of Nernst effect measurements taken from the system.

Nernst, Nernst effect, bismuth, bismuth telluride

# **Chapter 1. Introduction**

## **1.1. Introduction to Thermoelectric Materials**

Thermoelectric materials are materials which have the ability to convert heat into electrical energy, or vice versa. Thermoelectric materials thus have many applications in power generation or refrigeration devices. The efficiency of a thermoelectric material is described by its figure of merit, Z, which is given by (Rowe, 2006)

$$Z = \frac{S^2\sigma}{\lambda} \quad (1.1)$$

where S is the Seebeck coefficient,  $\sigma$  is the electrical conductivity, and  $\lambda$  is the thermal conductivity of the material. These coefficients and effects will be defined in greater detail in the following chapter. The quantity in the numerator of equation 1.1,  $S^2\sigma$ , is often called the power factor. Multiplying Z by the absolute temperature, T, gives a dimensionless figure of merit, ZT. For practical applications, ZT must be larger than 1, and the best thermoelectric materials currently known have a ZT only slightly larger than 1.

## **1.2. Goals**

The goal of the work presented in this thesis is to develop and construct a measuring system which will allow measurement of the Nernst effect for a given thermoelectric sample. The Nernst effect is not as well studied as other thermoelectric effects such as the Hall Effect or the Seebeck Effect, in part due to the difficulties in constructing a system to take the sensitive measurements required.

## Chapter 2. Background Theory

### 2.1. Overview of Thermoelectric Effects

#### 2.1.1. Electrical Conductivity

We open our discussion of thermoelectric effects with the simplest effect – that of electrical conductivity. Electrical conductivity (typically denoted by  $\sigma$ , although  $\kappa$  and  $\gamma$  are also used) represents the ability of a material to conduct electric current. Given a current density  $J$  and an electric field  $E$ , the electrical conductivity of the material is given as (Putley, 1960)

$$\sigma = \frac{J}{E} \quad (2.1)$$

$\sigma$  has units of Ampere/(Volt·Meter). Amperes per volt is often defined as siemens in SI units or “mhos” in electrical applications.

Conductivity is the inverse of resistivity – the ability of a material to resist current flow. Resistivity is typically denoted by  $\rho$  and is defined as (Putley, 1960)

$$\rho = \frac{1}{\sigma} = \frac{E}{J} \quad (2.2)$$

and has units of Ohm·Meters.

#### 2.1.2. The Seebeck Effect

As previously mentioned, thermoelectric materials allow the conversion of heat into electrical energy. When a temperature gradient is applied to the material, an electric current will be produced. This process is known as the Seebeck Effect, discovered in 1821 by Thomas Johann Seebeck. The Seebeck effect is closely linked to thermocouples. A thermocouple is an electrical device consisting of two different conductors. These conductors are connected in series, but held at different temperatures  $T_1$  and  $T_2$ . Under these conditions, a voltage  $V$  will develop between the contacts. Here, we have (Rowe, 2006)

$$V = S(T_1 - T_2) \quad (2.3)$$

where  $S$  is the Seebeck coefficient. Solving for the Seebeck coefficient gives (Rowe, 2006)

$$S = \frac{V}{\Delta T} \quad (2.4)$$

where  $\Delta T$  is the temperature gradient  $T_1 - T_2$ .  $S$  is positive if current flows in a clockwise direction and is often on the order of  $\mu\text{V/K}$ .

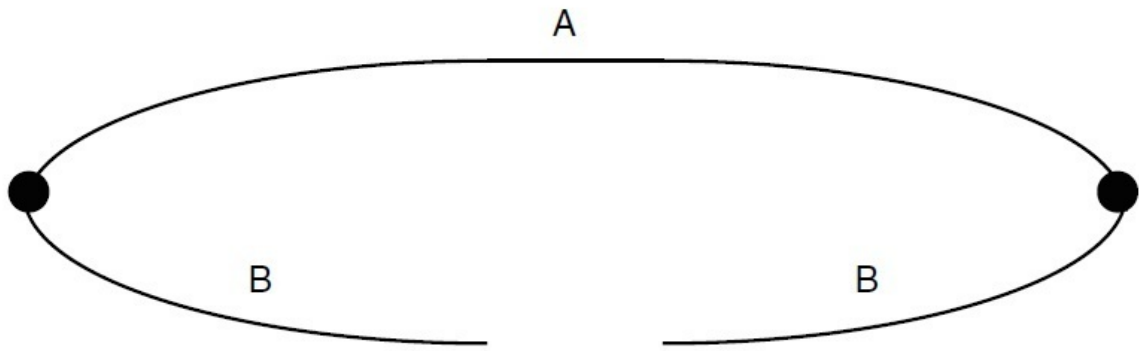


**Figure 2.1** A schematic of a simple thermocouple. "A" and "B" represent different materials. (Goldsmid, 2010)

### 2.1.3. *The Peltier Effect*

The Peltier Effect, named after French physicist Jean Charles Athanase Peltier who discovered it in 1834, is the inverse of the Seebeck Effect. If an external current source is applied between the two contacts of a thermocouple, heat will be generated between them. The Peltier coefficient,  $\pi$ , is defined as (Rowe, 2006)

$$\pi = \frac{I}{q} \quad (2.5)$$

where  $I$  is the current applied and  $q$  is the rate of heating.  $\pi$  is measured in Watts per Ampere, or Volts.

The following table serves to summarize the non-magnetic thermoelectric effects.

**Table 2.1 A summary of the non-magnetic thermoelectric effects.**

Experimental conditions	Resulting effect
I>0, ΔT=0	Electrical Conductivity, Peltier Effect
ΔT>0, I=0	Seebeck Effect

#### **2.1.4. The Hall Effect**

We begin discussion of the thermomagnetic effects with the Hall Effect. The Hall Effect, discovered in 1879 by Edwin Hall, allows us to determine the carrier type and concentration of carriers in a given sample. The Hall Effect is of particular importance in studying the Nernst Effect, as samples which give good Hall Effect measurements are ideal candidates for Nernst Effect measurements. The following derivation closely follows that in Sze and Ng (Sze, 2007).

Consider electrons (or holes) flowing in the x direction in a sample. In the absence of a magnetic field, these electrons will follow nearly straight paths through the sample. If a magnetic field is applied in the z direction, the electrons will curve downward into the y direction and accumulate on one side of the sample, leaving an absence of charge on the opposite side. This curvature of electrons is due to the Lorentz force,

$$F_B = qv_x \times B_z \quad (2.6)$$

At steady-state, the Lorentz force will be exactly balanced by the electric field created in the y direction,  $E_y$ . That is,

$$F_E = F_B \quad (2.7)$$

$$qE_y = qv_xB_z \quad (2.8)$$

This electric field can be referred to as the Hall field. The Hall voltage (the voltage in the y direction) can thus be given as

$$V_H = E_y W \quad (2.9)$$

where W is the width of the sample. We can also define the drift velocity of the electrons as

$$v_x = \frac{J}{ne} \quad (2.10)$$

where J is the current density, n is the carrier concentration, and e is the charge of the electron. J is defined as

$$J = \frac{I}{A} \quad (2.11)$$

where I is the current and A is the area of the sample. We thus can rewrite the drift velocity as

$$v_x = \frac{I}{Ane} \quad (2.12)$$

and we can then rewrite the Hall voltage as

$$V_H = v_x B_z W = \frac{IB_z W}{Ane} = \frac{IB_z}{tne} \quad (2.13)$$

where t is the thickness of the sample. We can also define the Hall coefficient as

$$R_H = \frac{E_y}{JB_z} = \frac{V_H}{WJB_z} = \frac{V_H A}{WIB_z} = \frac{V_H t}{IB_z} \quad (2.14)$$

The sign of the Hall coefficient denotes the majority carriers in the sample. For electrons (n-type material) the Hall coefficient is negative, whereas for holes (p-type material) the Hall coefficient is positive.  $R_H$  typically has units of  $\text{m}^3/\text{C}$  but is occasionally expressed in different units such as  $\Omega\cdot\text{cm}/\text{G}$ .

### **2.1.5. The Righi-Leduc Effect**

The Righi-Leduc Effect is a complete thermal analog of the Hall Effect (and is thus often called the Thermal Hall Effect). Given a magnetic field in the z direction and a temperature

gradient in the y direction, another temperature gradient will be produced in the x direction. The Righi-Leduc coefficient, A, is given as (Putley, 1960)

$$|A| = \frac{dT/dy}{B_z \cdot dT/dx} \quad (2.15)$$

#### **2.1.6. The Nernst Effect**

The Nernst Effect can be viewed as thermally analogous to the Hall Effect. Where electrons are driven by the Lorentz force in the Hall Effect, electrons are also driven by the temperature gradient present in the Nernst Effect. Electrons will diffuse from the hot side of the sample to the cold side in order to establish thermal equilibrium. Thermoelectric materials exhibit the Nernst Effect when they are subjected to a magnetic field ( $B_z$ ) and a temperature gradient ( $dT/dx$ ) at right angles to each other. Under these conditions, an electric field  $E_y$  will be produced which is perpendicular to both the temperature gradient and the magnetic field. A relationship between these quantities can be expressed in the Nernst coefficient, N (Rowe, 2006):

$$|N| = \frac{E_y/B_z}{dT/dx} \quad (2.16)$$

The Nernst effect is often referred to in literature as the First Nernst-Ettingshausen Effect, so named for its discoverers, Albert von Ettingshausen and his PhD student, Walther Nernst, who observed the effect in 1886 while studying the Hall Effect in Bismuth. Unlike the Hall Effect, the sign of N does not depend on the charge of the carriers in the material. N has units of V/(G·K).

#### **2.1.7. The Ettingshausen Effect**

The Ettingshausen Effect, or the Second Nernst-Ettingshausen Effect, can be viewed as an inverse to the Nernst Effect. Given a magnetic and electric field applied perpendicular to each

other, a temperature gradient will be produced perpendicular to both the magnetic and electric fields. This effect is quantified in the Ettingshausen coefficient, P (Rowe,2006):

$$|P| = \frac{dT/dx \cdot d_z}{B_z * I_y} \quad (2.17)$$

Where  $d_z$  is the thickness of the sample and  $I_y$  is the current applied to the sample. P has units of K/(G·A).

There is a thermodynamic relationship between the Ettingshausen coefficient and the Nernst coefficient which can be expressed as (Goldsmid, 2010)

$$P\lambda = NT \quad (2.18)$$

Here, as in equation 1.1,  $\lambda$  is the thermal conductivity. The thermal conductivity is included in the relationship since the Nernst and Ettingshausen effects are defined in terms of a temperature gradient rather than heat flow.

Figure 2.2 and the following table summarize the thermomagnetic effects.

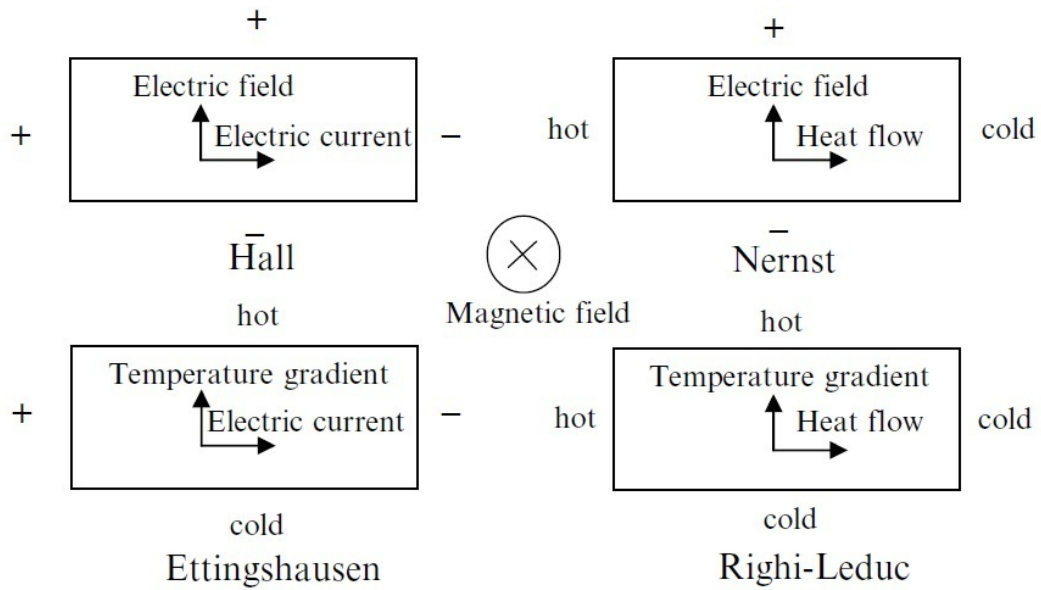


**Figure 2.2.** A visual summary of the thermomagnetic effects. Coefficients are positive when the effects are in the directions shown in the diagram (Goldsmid, 2010).

**Table 2.2.** A summary of the thermomagnetic effects.  $\Delta T$  is the temperature difference,  $B$  is the magnetic field and  $I$  is electrical current.

Experimental Conditions	Resulting Effect
$\Delta T=0; B>0; I=0$	Hall Effect
$\Delta T>0; B>0; I=0$	Nernst Effect, Righi-Leduc Effect
$\Delta T=0; B>0; I>0.$	Ettingshausen Effect

## Chapter 3. Experimental Setup

### 3.1. Equipment

In order to take Nernst Effect measurements, we need to apply both a magnetic field and a temperature gradient across the sample. We use a GMW 3742 Dipole Electromagnet together

with a GMW System 8500 Magnet Power Supply in order to generate a magnetic field. This field is measured using a LakeShore 455 DSP Gaussmeter. We create a temperature gradient across the sample by powering a  $100\ \Omega$  resistor attached to the sample to generate heat. This resistor is powered by a Kiethley 6221 AC/DC current source. We take voltage readings using Kiethley 2182A Nanovoltmeters. We use four nanovoltmeters total. Two of the nanovoltmeters are set up to read voltages across the sample. The other two nanovoltmeters take voltage readings from the thermocouples connected to the sample. We also use a Lakeshore 331S Temperature Controller to read the base temperature. All instruments are connected to the computer via GPIB, or General Purpose Information Bus. Connecting the instruments through GPIB allows programs such as LabView to interface with the instruments easily.



**Figure 3.1. Nernst effect measuring system in our lab.**

### 3.2. Sample Setup

Voltage leads are soldered directly to the sample as shown in the diagram below.

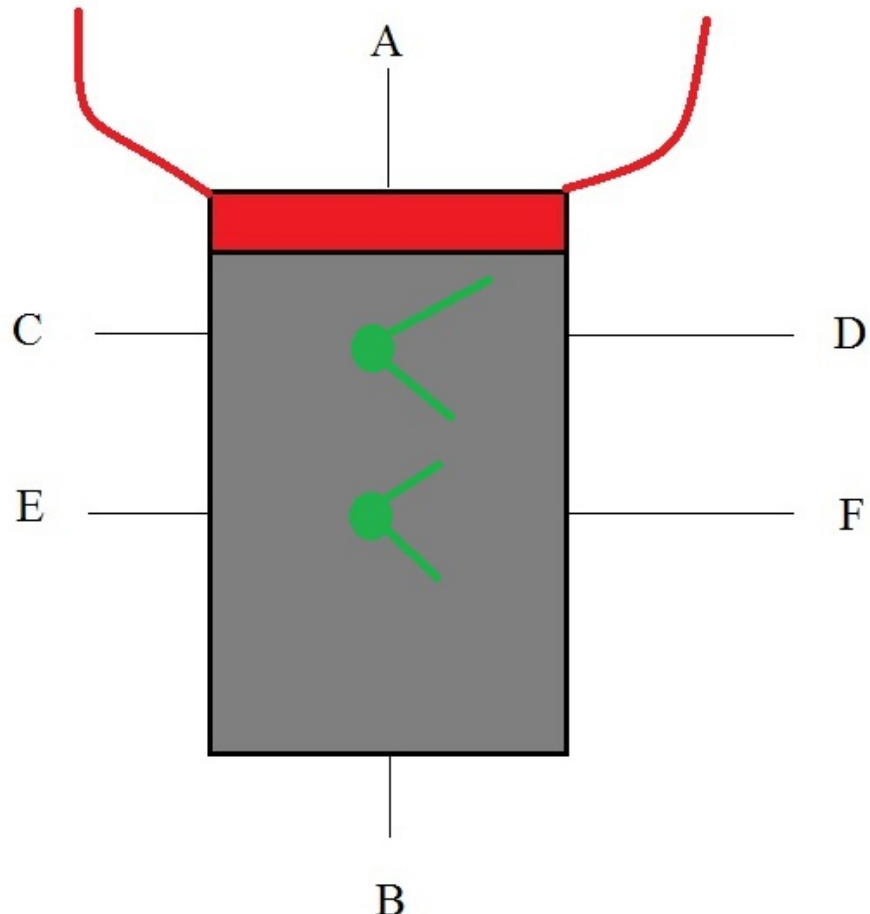


**Figure 3.2.** A diagram showing the position of leads on the sample. The red wires represent leads to power the heater. The green wires are thermocouple leads.

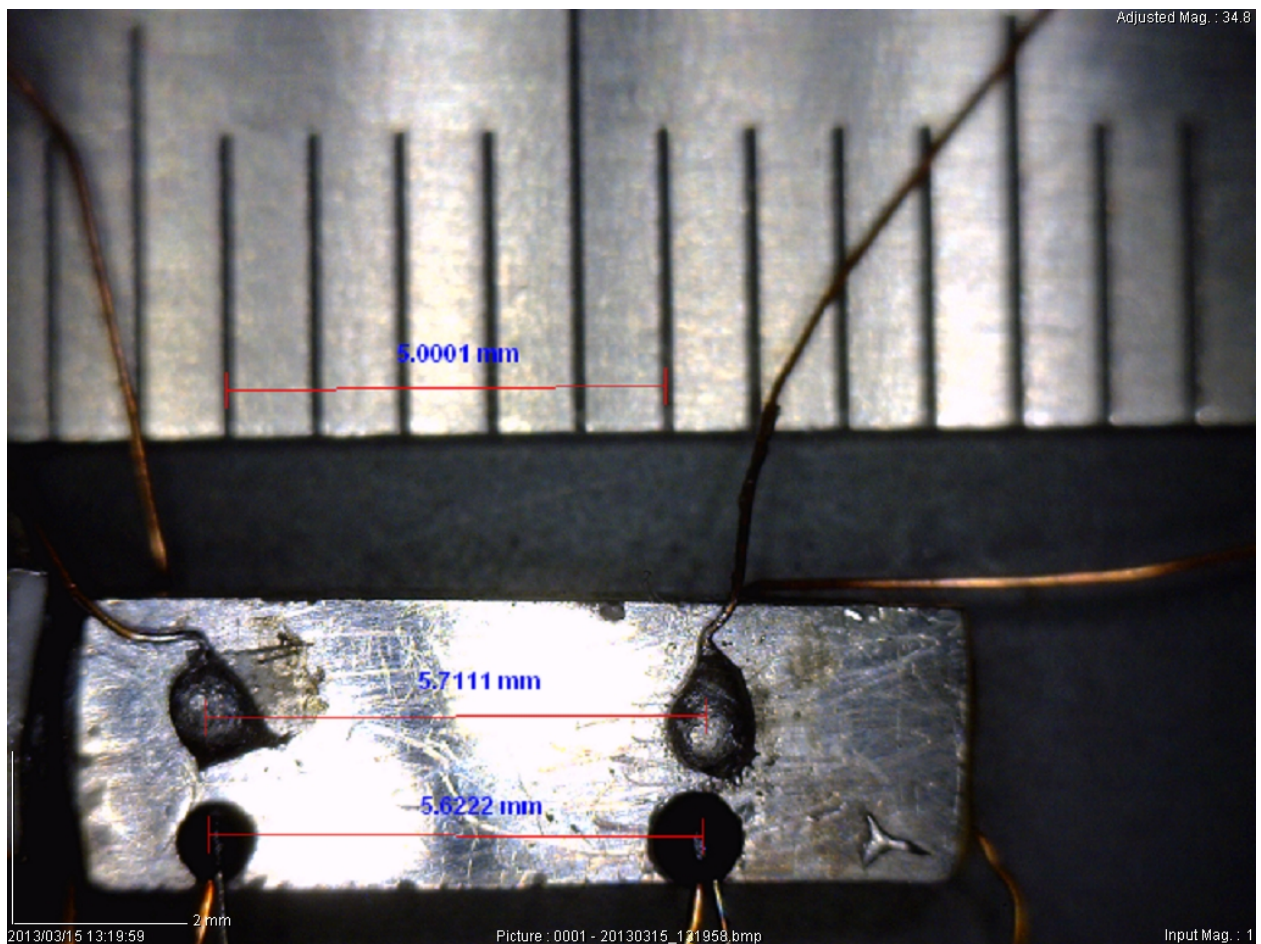


**Figure 3.3. A photograph showing thermocouple and voltage leads attached to the sample.**

Thermocouple leads are connected to the sample using Styccast. Styccast is an adhesive which has excellent thermal conductivity and is electrically insulating. The sample is then mounted in the chamber. Once the sample is mounted, the leads can be soldered onto the neighboring pins, which connect it to the measuring system as shown below.

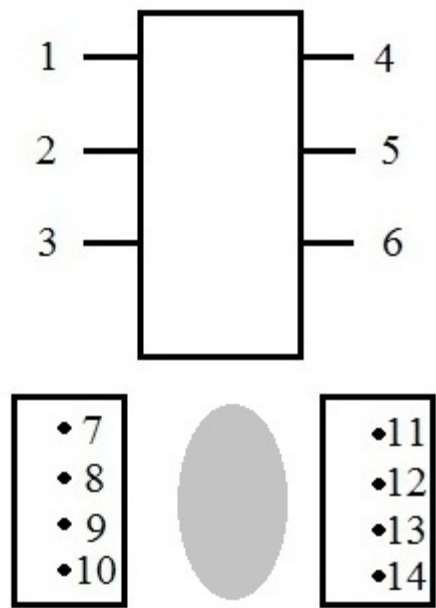


**Figure 3.4.** A schematic diagram showing how the sample is connected to the various measuring instruments. The gray oval represents the sample holder and thermocouple stage. The connections are as follows:

- 1: I+, KE6221
- 2: BNC "D" lead
- 3: BNC "C" lead
- 4: I-, KE6221
- 5: Top Thermocouple Copper ( $V_1^+$ )
- 6: BNC "A" lead
- 7: Top Thermocouple Constantan ( $V_1^-$ )
- 8: BNC "F" lead
- 9: BNC "E" lead
- 10: Empty
- 11: BNC "B" lead
- 12: Empty
- 13: Bottom Thermocouple Copper ( $V_2^+$ )
- 14: Bottom Thermocouple Constantan ( $V_2^-$ )

Thermocouple connections are routed through the 10-pin connector to the appropriate KE2182A nanovoltmeters.

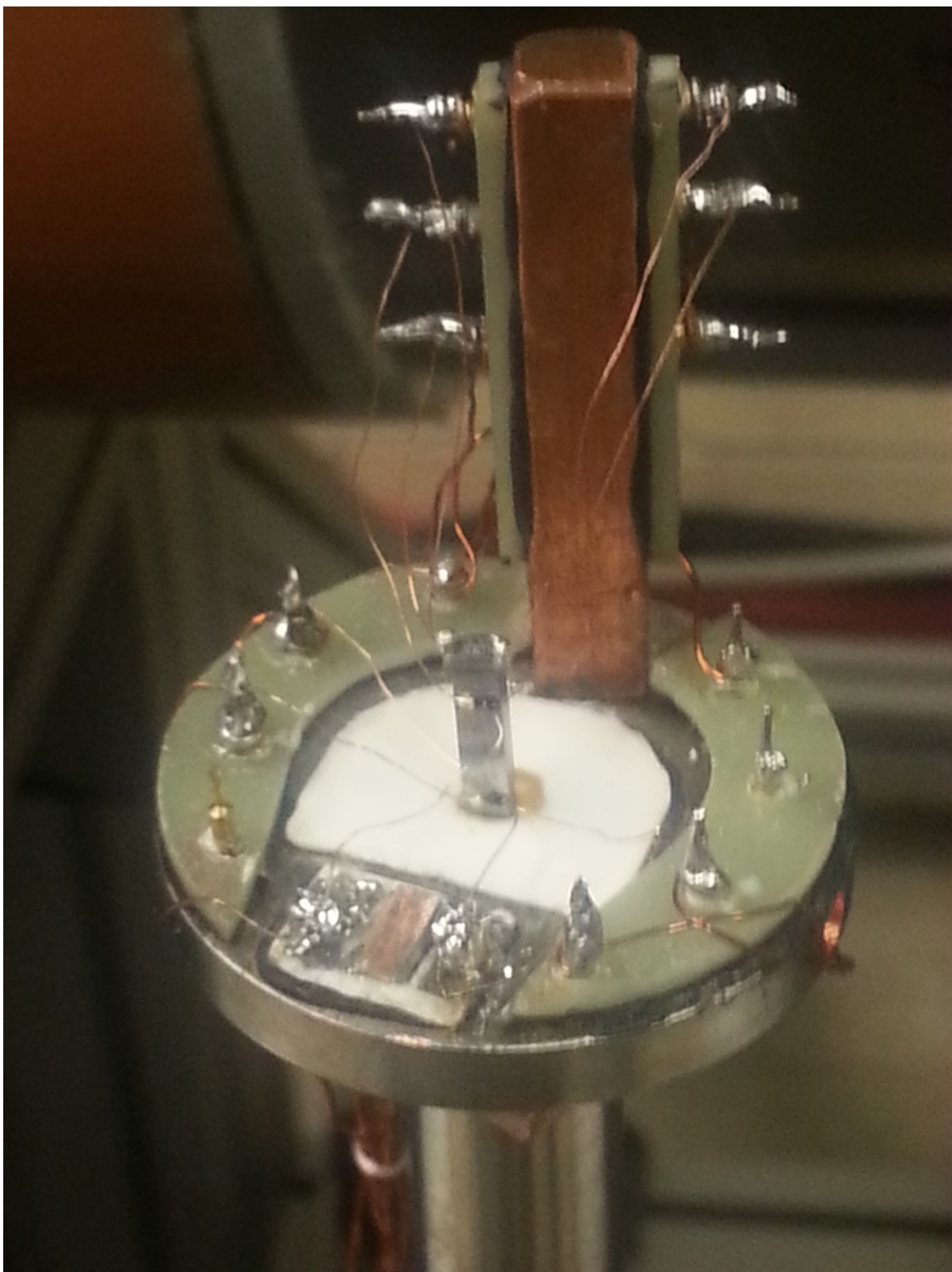


**Figure 3.5.** A sample mounted in the chamber.

The BNC cables are connected to a converter box which we constructed in order to connect the BNC cables to the nanovoltmeters. The converter box also was designed with a slot for a 25-pin connector for connection to a LakeShore 370 AC Resistance Bridge. This allows us to make Hall Effect measurements in the future using the already existing system. The 25 pin connector will connect to BNC leads “A” and “B”, which are currently not used.

### **3.3. LabView Program Design**

Before writing LabView programs to take measurements from the sample, it was necessary to design a program to control our electromagnet’s magnetic field. Designing this program proved to be a unique challenge. Our goal was to create a program that would allow the user to input a desired field and a tolerance, and quickly reach the inputted field. Both speed and precision are important – our measurements require a tolerance of 1 Gauss. A program was provided with the electromagnet, but we quickly realized that it was far too imprecise for our measurements. In addition, there was no way to automate this program, which would require us to manually set each field value, making measurements take a very long time. After studying the stock control program, we learned that the magnet is actually controlled by sending a current value to the electromagnet via GPIB. The magnet then passes that much current through it and produces a magnetic field accordingly. We took a graph of inputted current vs. outputted field and found a nearly linear relationship, with a small amount of hysteresis present in the electromagnet. Thus, a program that simply stored current values for different field values would not work – it would additionally matter which direction a value was being approached from, making such a program far too complicated. We used the slope of this current vs. magnetic field line (in units of Gauss/Ampere) as the basis for an algorithm to quickly set field values. The program to set the magnetic field works as follows:

- 1) First, take a reading from the Gaussmeter to determine if the existing field is already within tolerance of the desired field. This serves as a sanity check and prevents us from wasting time trying to reach an already set field.
- 2) Next, we read the amount of current already being passed through the magnet. This determines our starting point.
- 3) Take a reading from the Gaussmeter and subtract the reading from the desired field. Dividing this by the slope of the line tells us how many additional amps of current need to be added in order to reach the desired field.
- 4) Add that much current to the current already present. Pass that amount of current. Take a reading from the Gaussmeter. If the reading is within tolerance, stop. If not, return to step 3.

This program works equally well for positive and negative field values. The magnet will automatically interpret negative current values as reversed polarity, eliminating the need to manually switch the magnet's polarity. However, special care must be taken when trying to set the field to zero. The program requires longer waits in between steps when trying to reach zero, otherwise the magnet's power supply will shut itself off. We believe this is caused by a bug in the power supply's handling of small current values.

### **3.4. Taking Measurements**

We can take measurements in two different ways. We can hold either the magnetic field constant and vary temperature or hold the temperature gradient constant and vary magnetic field. Two separate programs were written for this purpose; one for varying magnetic field and one for varying temperature gradient. In varying the magnetic field experiment, we typically record voltage values for fields ranging from -5000 Gauss to 5000 Gauss, in 500 Gauss steps. To vary

the temperature gradient, we vary the current, and thus, the power, supplied to the resistor on the sample. For example, a typical measurement profile would be from 22 mA to 28 mA, in 2 mA increments. Since  $P = I^2R$ , where  $R= 100 \Omega$ , the power supplied to the resistor ranges from 48.4 to 78.4 mW.

At each magnetic field or current value, we take a number of voltage readings (typically 20) from across the sample (C/D and E/F in Figure 2.2) and average them. We then record these averages in a text file, along with the standard deviation and variance for each reading. This process is then repeated for all magnetic field or current values. The data is then tabulated in Origin 8.0. We expect that plots of magnetic field or temperature gradient vs. C/D and E/F voltage will produce a straight line.

### 3.5. Approximations for the Nernst Coefficient

Additionally, we must relate the Nernst coefficient to the known and measured quantities we have. We previously defined the Nernst coefficient as (Rowe, 2006):

$$|N| = \frac{E_y/B_z}{dT/dx} \quad (2.16)$$

We need to employ some algebraic manipulation in order to describe N in terms of our known quantities. First, we will approximate  $dT/dx$  as:

$$\frac{dT}{dx} \approx \frac{\Delta T}{l} \quad (3.1)$$

Here,  $l$  is the distance between the two thermocouples and  $\Delta T=T_2-T_1$ , where  $T_1$  and  $T_2$  are the temperatures at the thermocouples. Since we cannot directly measure the temperatures at the thermocouples, we must again employ an approximation using the base temperature,  $T_0$ , the sensitivity at the base,  $S(T_0)$ , and the voltage measured from the thermocouples,  $V$ . We can thus approximate the temperature at a thermocouple as:

$$T_1 \approx \frac{V_1}{S(T_0)} + T_0 \quad (3.2)$$

$$T_2 \approx \frac{V_2}{S(T_0)} + T_0 \quad (3.3)$$

Combining 2.2 and 2.3 gives an expression for  $\Delta T$ :

$$\Delta T = \frac{V_2}{S(T_0)} + T_0 - \frac{V_1}{S(T_0)} - T_0$$

$$\Delta T = \frac{V_2 - V_1}{S(T_0)} \quad (3.4)$$

We will also let  $E=V/d$ , where  $d$  is the thickness of the sample. Substituting into our expression for  $N$  gives:

$$N = \frac{V/(dB)}{\Delta T/l} = \frac{Vl}{dB\Delta T} \quad (3.5)$$

If we are taking a measurement at constant temperature gradient (i.e., varying the magnetic field), the slope of the line plotted in Origin is:

$$m_{mag} = \frac{V}{B} \quad (3.6)$$

so our expression for  $N$  becomes:

$$N = \frac{lm_{mag}}{d\Delta T} \quad (3.7)$$

If we instead are taking measurements at constant magnetic field, the slope of the line is:

$$m_{temp} = \frac{V}{\Delta T} \quad (3.8)$$

and our expression for  $N$  is:

$$N = \frac{lm_{temp}}{dB} \quad (3.9)$$

$N$  is now completely in terms of known parameters: the thickness of the sample ( $d$ ), the distance between thermocouples ( $l$ ), the magnetic field strength ( $B$ ), the temperature difference between the two thermocouples ( $\Delta T$ ), and the voltage ( $V$ ).

## Chapter 4. Results

We measured two different samples in order to test our measuring system: bismuth nickel telluride (BiNiTe) and bismuth antimony telluride (BiSbTe). We measured each sample at both constant temperature and at constant magnetic field. Results for each sample are listed in the following tables. Raw data and graphs for BiNiTe at constant temperature gradient follows:

Magnetic Field (G)	E/F Voltage (V)	C/D Voltage (V)	Bot TC Volt (V)	Top TC Volt (V)
-5000.000	1.50772E-04	-3.87966E-04	3.73686E-04	8.03590E-04
-4501.000	1.51376E-04	-3.87080E-04	3.73669E-04	8.03629E-04
-4000.800	1.51939E-04	-3.86196E-04	3.73644E-04	8.03656E-04
-3500.900	1.52486E-04	-3.85358E-04	3.73631E-04	8.03689E-04
-3000.600	1.53115E-04	-3.84377E-04	3.73639E-04	8.03769E-04
-2500.280	1.53732E-04	-3.83491E-04	3.73653E-04	8.03864E-04
-2000.320	1.54346E-04	-3.82650E-04	3.73692E-04	8.03991E-04
-1500.320	1.54962E-04	-3.81755E-04	3.73724E-04	8.04124E-04
-1000.910	1.55520E-04	-3.80867E-04	3.73731E-04	8.04220E-04
-500.460	1.56150E-04	-3.79915E-04	3.73722E-04	8.04283E-04
0.179	1.56788E-04	-3.79008E-04	3.73680E-04	8.04304E-04
499.250	1.57433E-04	-3.78141E-04	3.73683E-04	8.04413E-04
999.300	1.58088E-04	-3.77255E-04	3.73683E-04	8.04494E-04
1499.250	1.58674E-04	-3.76394E-04	3.73686E-04	8.04579E-04
1999.680	1.59266E-04	-3.75519E-04	3.73648E-04	8.04600E-04
2499.200	1.59906E-04	-3.74595E-04	3.73585E-04	8.04600E-04
2999.600	1.60566E-04	-3.73697E-04	3.73525E-04	8.04604E-04
3499.000	1.61123E-04	-3.72838E-04	3.73485E-04	8.04638E-04
3999.600	1.61764E-04	-3.71919E-04	3.73386E-04	8.04581E-04
4499.200	1.62316E-04	-3.70993E-04	3.73250E-04	8.04457E-04
4999.900	1.62968E-04	-3.70109E-04	3.73037E-04	8.04270E-04

Bot TC Temp (K)	Top TC Temp (K)	E/F Std. Dev.	C/D Std. Dev.	Bot TC Volt S.Dev	Top TC Volt S.Dev
9.18148	19.74423	7.36088E-09	1.63787E-08	2.67474E-09	6.30359E-09
9.18105	19.74518	7.13477E-09	8.04861E-09	3.32941E-09	4.63078E-09
9.18044	19.74584	1.04673E-08	2.27347E-08	3.93667E-09	3.30917E-09
9.18013	19.74667	1.01242E-08	2.35184E-08	2.26804E-09	7.35335E-09
9.18032	19.74862	9.09288E-09	5.54190E-09	2.98171E-09	7.81865E-09
9.18066	19.75096	2.26565E-08	2.25838E-08	2.27495E-09	1.15804E-08
9.18162	19.75408	1.95194E-08	2.89690E-08	3.92680E-09	1.00266E-08
9.18242	19.75734	2.20386E-08	1.77580E-08	1.94140E-09	1.03291E-08
9.18259	19.75971	1.89738E-08	1.49314E-08	1.43065E-09	7.38828E-09
9.18236	19.76125	8.81285E-09	1.48472E-08	3.13079E-09	1.96369E-09
9.18133	19.76177	3.10906E-08	8.80664E-09	1.34668E-09	7.59526E-09
9.18141	19.76444	6.96927E-09	1.90104E-08	3.21239E-09	8.55880E-09
9.18140	19.76643	1.11154E-08	9.12973E-09	2.23914E-09	4.83699E-09
9.18148	19.76852	1.25650E-08	1.45521E-08	3.50829E-09	7.16641E-09
9.18053	19.76905	3.04623E-08	6.76748E-09	7.64242E-09	2.33880E-09
9.17900	19.76904	1.19045E-08	1.05973E-08	5.75594E-09	3.10762E-09
9.17752	19.76915	1.37534E-08	1.36950E-08	5.43965E-09	2.29926E-09
9.17653	19.76998	1.05893E-08	5.54475E-09	8.53890E-09	3.94580E-09
9.17411	19.76859	2.17142E-08	7.36793E-09	1.25408E-08	8.79799E-09
9.17076	19.76554	2.33446E-08	1.45795E-08	1.58085E-08	1.88983E-08
9.16554	19.76093	2.57276E-08	1.20291E-08	3.98324E-08	4.87161E-08

**Figure 4.1. Raw data for BiNiTe sample at constant temperature gradient. Note: Bot TC Temp and Top TC Temp values are the temperature difference from the base temperature, not the absolute temperature at the thermocouple. LabView carries out this calculation autom**

Current Level (mA): 25

Base Temperature (K): 2.968200E+2

Sample TC Length (mm): 5.6222

Sample Thickness (mm): 2.44

Average Bottom Temperature Difference (K): 9.17918

Average Top Temperature Difference (K): 19.7594

Temperature Gradient across sample (K/mm): 1.88186

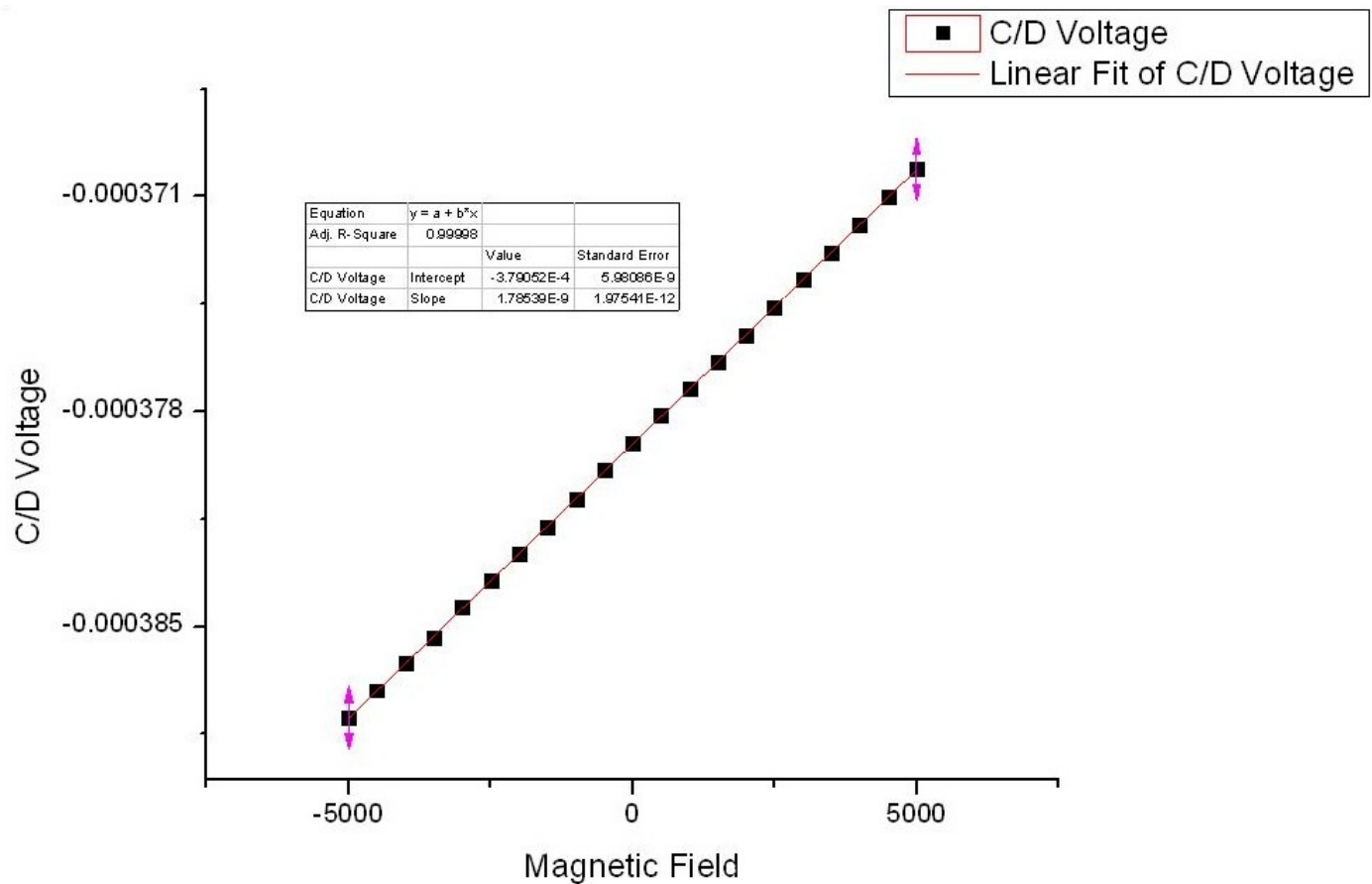
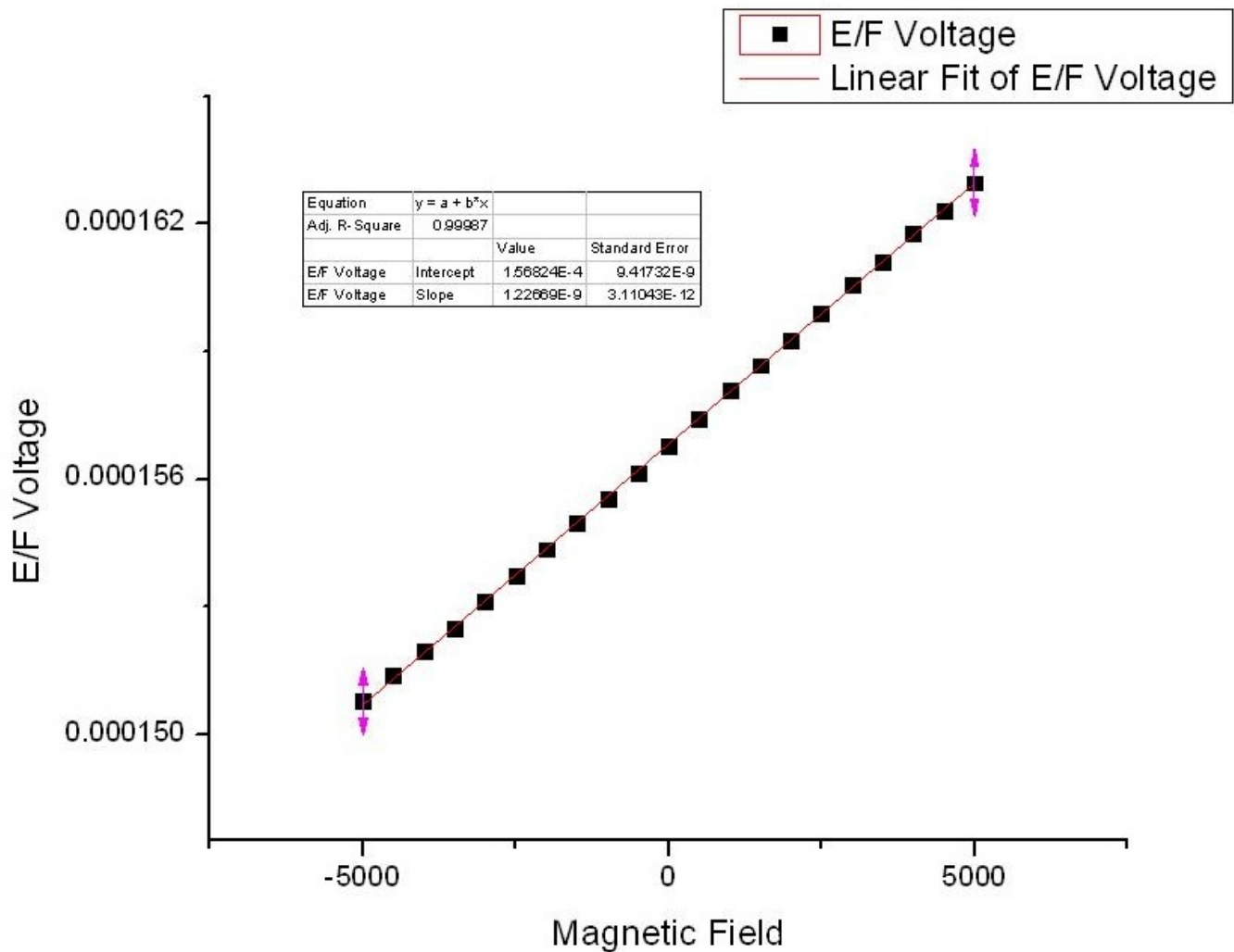


Figure 4.2. Plot of C/D Voltage vs. Magnetic Field for BiNiTe sample.



**Figure 4.3. Plot of E/F Voltage vs. Magnetic Field for BiNiTe sample**

Using equation 3.7 and using the E/F slope gives a Nernst coefficient of  $2.6714 \times 10^{-10}$  V/(K·G), or  $2.6714 \times 10^{-6}$  V/(K·T). The same calculation using the C/D slope instead gives a Nernst coefficient of  $3.8881 \times 10^{-10}$  V/(K·G), or  $3.881 \times 10^{-6}$  V/(K·T).

Raw data and graphs for BiNiTe at constant magnetic field follows:

Current (mA)	E/F Voltage (V)	C/D Voltage (V)	Top TC Voltage (V)	Bot TC Voltage (V)	E/F Volt S. Dev	C/D Volt S. Dev
22	1.27E-04	-2.98E-04	6.18E-04	2.87E-04	1.65E-08	7.98E-08
24	1.49E-04	-3.46E-04	7.38E-04	3.43E-04	5.39E-08	5.78E-08
26	1.74E-04	-3.94E-04	8.69E-04	4.05E-04	5.68E-08	6.35E-08
28	1.99E-04	-4.42E-04	0.00101	4.71E-04	1.70E-08	5.37E-08

Top TC Volt S. Dev	Bot TC Volt S. Dev	Top Delta T(K)	Bot Delta T(K)	Base Temp(K)	Delta T (K)	Temp Gradient (K/mm)
4.30E-07	2.80E-07	15.19458	7.04637	296.77	8.14821	1.44934402
4.32E-07	2.86E-07	18.1422	8.43144	296.8	9.71076	1.72727825
4.64E-07	3.10E-07	21.34574	9.94052	296.83	11.40522	2.02867714
4.66E-07	3.21E-07	24.79504	11.56905	296.87	13.22599	2.35254198

Figure 4.4. Raw data for BiNiTe sample at constant magnetic field.

Magnetic Field: 5000 G = 0.5 T

Base Temperature (K): 296.8200

Sample TC Length (mm): 5.6222

Sample Thickness (mm): 2.44

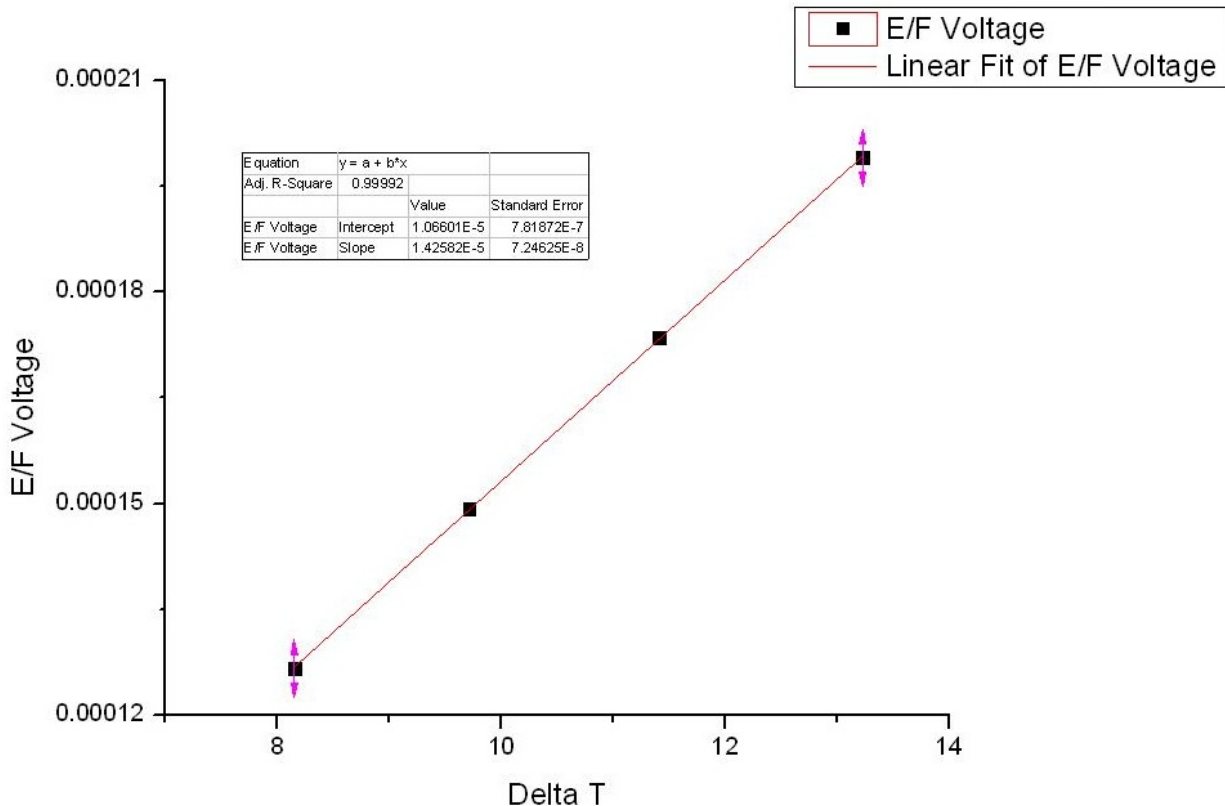
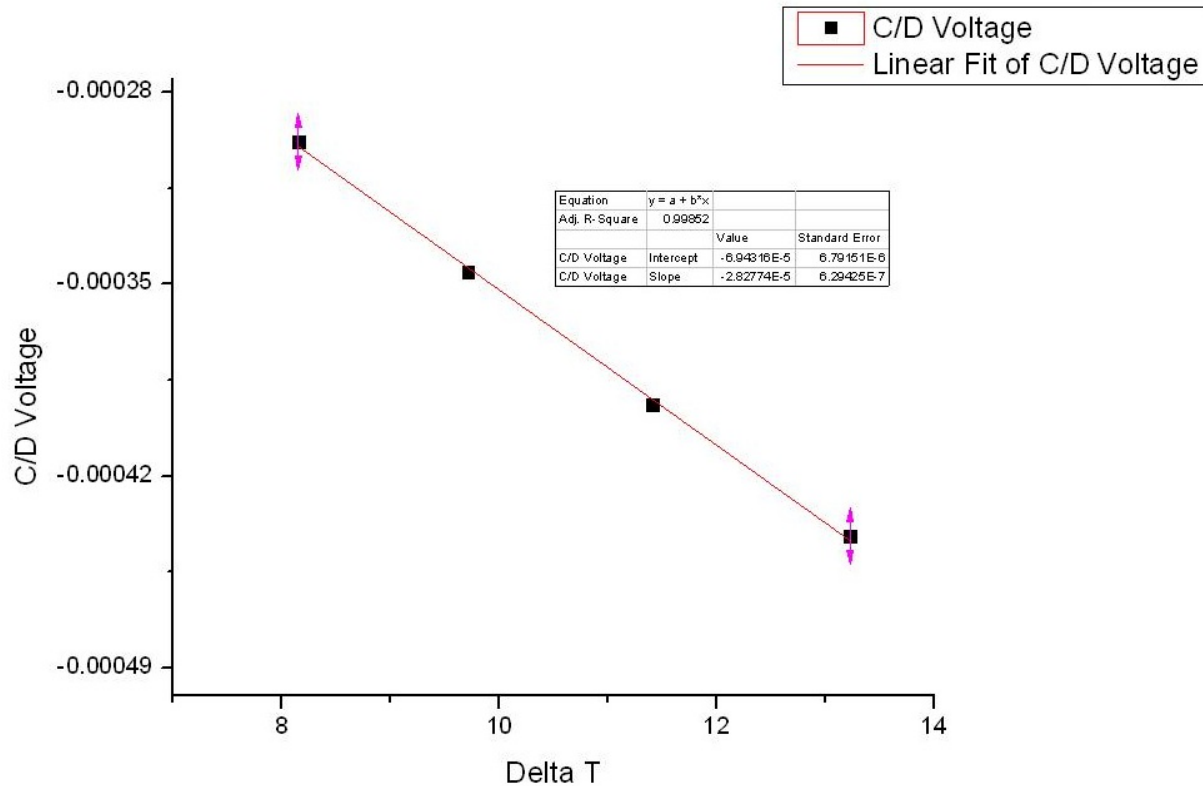


Figure 4.5. Plot of E/F Voltage vs.  $\Delta T$  for BiNiTe sample at constant 5000G field.



**Figure 4.6. Plot of C/D Voltage vs.  $\Delta T$  for BiNiTe sample at 5000G magnetic field.**

It is important to note in Figure 3.6 that, although the voltage is becoming more negative, the magnitude of the voltage is the important quantity. The magnitude of the voltage is increasing with increasing temperature gradient, which agrees with theory.

Using equation 3.9 and the E/F slope gives a Nernst coefficient of  $6.5713 \cdot 10^{-9}$  V/(K·G), or  $6.5713 \cdot 10^{-5}$  V/(K·T). Using the C/D slope gives a coefficient of  $1.3027 \cdot 10^{-8}$  V/(K·G), or  $1.3027 \cdot 10^{-4}$  V/(K·T).

Raw data and graphs for BiSbTe at constant temperature gradient follow.

Magnetic Field (G)	E/F Voltage (V)	C/D Voltage (V)	Bot TC Voltage (V)	Top TC Voltage (V)	Bot TC Temp (K)	Top TC Temp (K)
5000.20	-3.68E-04	-8.79E-05	1.87E-04	1.10E-03	4.57E+00	2.71E+01
4499.70	-3.68E-04	-8.69E-05	1.87E-04	1.10E-03	4.57E+00	2.71E+01
3999.60	-3.67E-04	-8.56E-05	1.87E-04	1.10E-03	4.57E+00	2.71E+01
3499.10	-3.66E-04	-8.60E-05	1.87E-04	1.10E-03	4.57E+00	2.71E+01
2999.70	-3.66E-04	-8.60E-05	1.87E-04	1.10E-03	4.57E+00	2.71E+01
2499.50	-3.65E-04	-8.53E-05	1.87E-04	1.10E-03	4.57E+00	2.71E+01
1999.80	-3.65E-04	-8.41E-05	1.87E-04	1.10E-03	4.57E+00	2.71E+01
1499.45	-3.64E-04	-8.37E-05	1.87E-04	1.10E-03	4.57E+00	2.71E+01
999.42	-3.63E-04	-8.29E-05	1.87E-04	1.10E-03	4.57E+00	2.71E+01
499.40	-3.63E-04	-8.25E-05	1.87E-04	1.10E-03	4.57E+00	2.71E+01
0.69	-3.63E-04	-8.30E-05	1.87E-04	1.10E-03	4.57E+00	2.71E+01
-500.72	-3.62E-04	-8.14E-05	1.87E-04	1.10E-03	4.57E+00	2.71E+01
-1000.82	-3.62E-04	-8.04E-05	1.86E-04	1.10E-03	4.57E+00	2.71E+01
-1500.97	-3.61E-04	-8.01E-05	1.86E-04	1.10E-03	4.57E+00	2.70E+01
-2000.98	-3.60E-04	-7.94E-05	1.86E-04	1.10E-03	4.57E+00	2.70E+01
-2500.26	-3.60E-04	-7.87E-05	1.87E-04	1.10E-03	4.57E+00	2.70E+01
-3000.60	-3.59E-04	-7.77E-05	1.87E-04	1.10E-03	4.57E+00	2.71E+01
-3500.70	-3.59E-04	-7.71E-05	1.87E-04	1.10E-03	4.57E+00	2.71E+01
-4000.10	-3.58E-04	-7.59E-05	1.87E-04	1.10E-03	4.57E+00	2.70E+01
-4500.80	-3.58E-04	-7.55E-05	1.87E-04	1.10E-03	4.57E+00	2.70E+01
-4999.70	-3.57E-04	-7.46E-05	1.87E-04	1.10E-03	4.57E+00	2.70E+01

E/F Std. Dev.	C/D Std. Dev	Bot TC Volt S.Dev	Top TC Volt S.Dev
7.12E-09	9.32E-08	5.75E-09	1.89E-08
1.42E-08	2.37E-07	3.49E-09	1.08E-08
1.59E-08	1.35E-07	2.38E-09	3.29E-09
9.05E-09	1.76E-07	6.64E-09	1.72E-08
5.09E-09	1.39E-07	4.00E-09	1.19E-08
1.51E-08	1.61E-07	3.01E-09	1.32E-08
1.08E-08	2.56E-07	2.20E-09	4.59E-09
1.67E-08	1.19E-07	1.97E-09	5.83E-09
1.95E-08	1.09E-07	5.87E-09	1.81E-08
1.31E-08	1.85E-07	2.98E-09	1.04E-08
1.27E-08	4.12E-07	7.64E-09	4.01E-08
9.48E-09	1.23E-07	4.31E-09	6.97E-09
1.35E-08	2.36E-07	9.33E-09	2.31E-08
9.41E-09	2.15E-07	4.78E-09	1.70E-08
1.02E-08	1.82E-07	1.05E-09	3.21E-09
9.08E-09	1.39E-07	4.99E-09	9.68E-09
1.25E-08	1.04E-07	2.25E-09	2.86E-09
9.15E-09	1.98E-07	4.71E-09	1.23E-08
1.41E-08	3.19E-07	2.23E-09	2.76E-09
9.50E-09	1.14E-07	1.52E-09	3.61E-09
1.18E-08	1.67E-07	8.23E-09	1.87E-08

**Figure 4.7. Raw data for BiSbTe sample at constant temperature gradient**

Current Level (mA): 25  
 Base Temperature(K): 298.35  
 Current Level (mA): 25  
 Sample TC Length (mm): 6.7858  
 Sample Thickness (mm): 2.38  
 Average Bot Temperature  
 Difference (K): 4.57  
 Average Top Temperature  
 Difference (K): 27.1  
 Temperature Gradient across  
 sample: 3.3135 K/mm

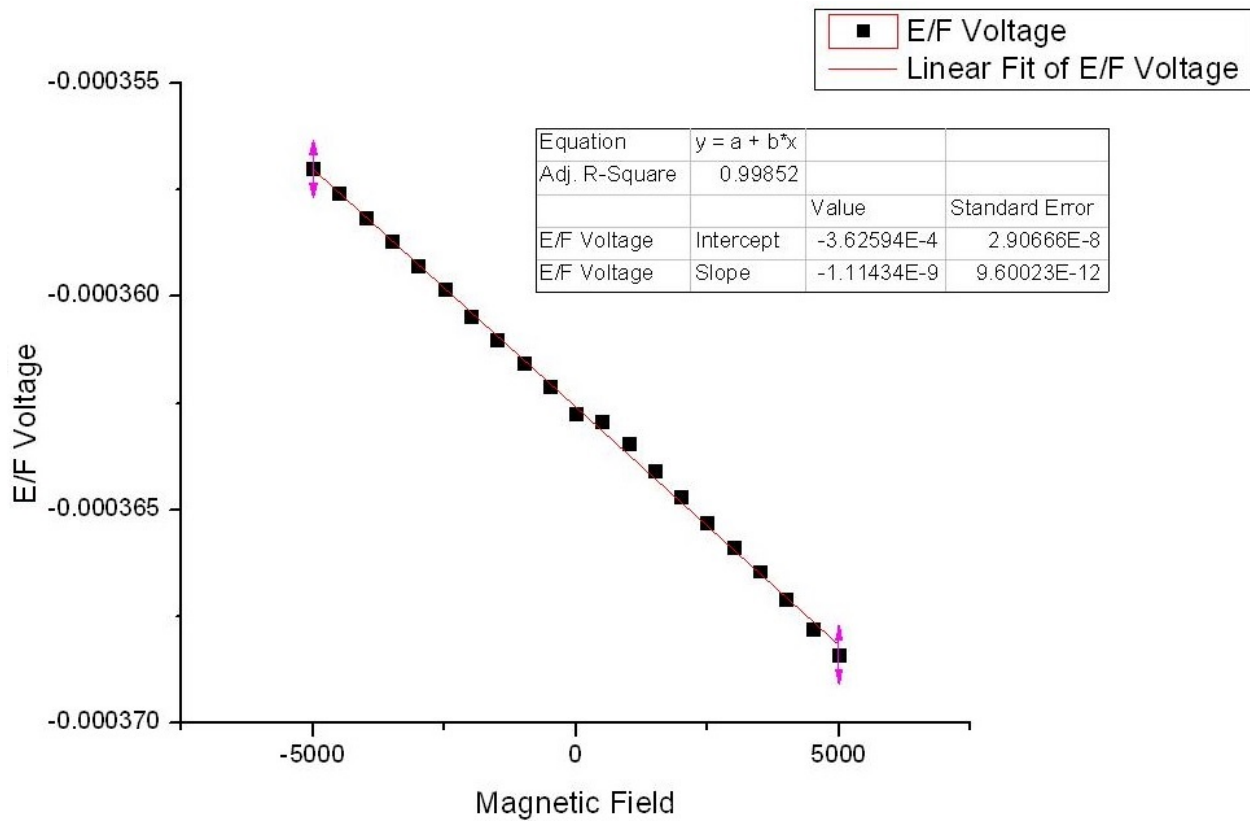
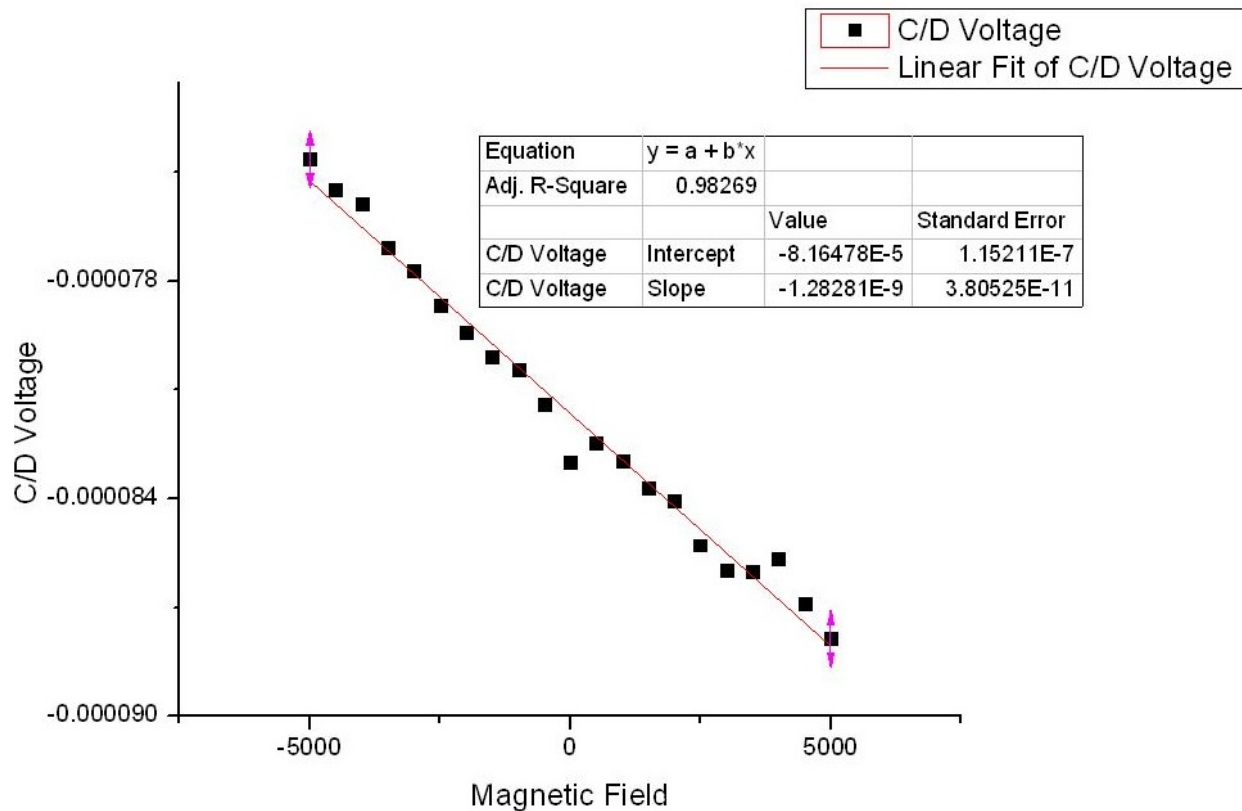


Figure 4.8. Graph of E/F Voltage vs. Magnetic Field for BiSbTe sample.



**Figure 4.9. Graph of C/D Voltage vs. Magnetic Field for BiSbTe sample.**

Using equation 3.7 and using the E/F Slope gives a Nernst coefficient of  $1.4101 \times 10^{-10}$  V/(G·K), or  $1.4101 \times 10^{-6}$  V/(T·K). Using the C/D Slope instead gives a Nernst coefficient of  $1.6234 \times 10^{-10}$  V/(G·K), or  $1.6234 \times 10^{-6}$  V/(T·K).

Raw data and graphs for BiSbTe sample at constant magnetic field follows.

Current (mA)	E/F Voltage (V)	C/D Voltage (V)	Top TC Voltage (V)	Bot TC Voltage (V)	E/F Volt S. Dev	C/D Volt S. Dev
22.00	-2.82E-04	-6.90E-05	8.57E-04	1.47E-04	1.82E-07	3.85E-07
24.00	-3.35E-04	-8.29E-05	1.02E-03	1.74E-04	2.36E-07	2.48E-07
26.00	-3.91E-04	-1.00E-04	1.20E-03	2.04E-04	2.52E-07	1.69E-07
28.00	-4.53E-04	-1.18E-04	1.39E-03	2.35E-04	2.60E-07	3.73E-07

Top TC Volt S. Dev	Bot TC Volt S. Dev	Top Delta T(K)	Bot Delta T(K)	Base Temp(K)	Delta T (K)	Temperature Gradient (K/mm)
6.31E-07	1.60E-07	21.01	3.60	2.98E+02	17.41	2.565677326
6.49E-07	1.66E-07	25.03	4.27	2.98E+02	20.76	3.059532597
7.09E-07	1.77E-07	29.40	4.99	2.98E+02	24.41	3.5970663
7.37E-07	1.82E-07	34.12	5.76	2.98E+02	28.36	4.178683442

**Figure 4.10. Raw data for BiSbTe sample at constant magnetic field.**

Magnetic Field: 5000 G = 0.5 T  
Base Temperature (K): 298.00  
Sample TC Length (mm): 6.7858  
Sample Thickness (mm): 2.38

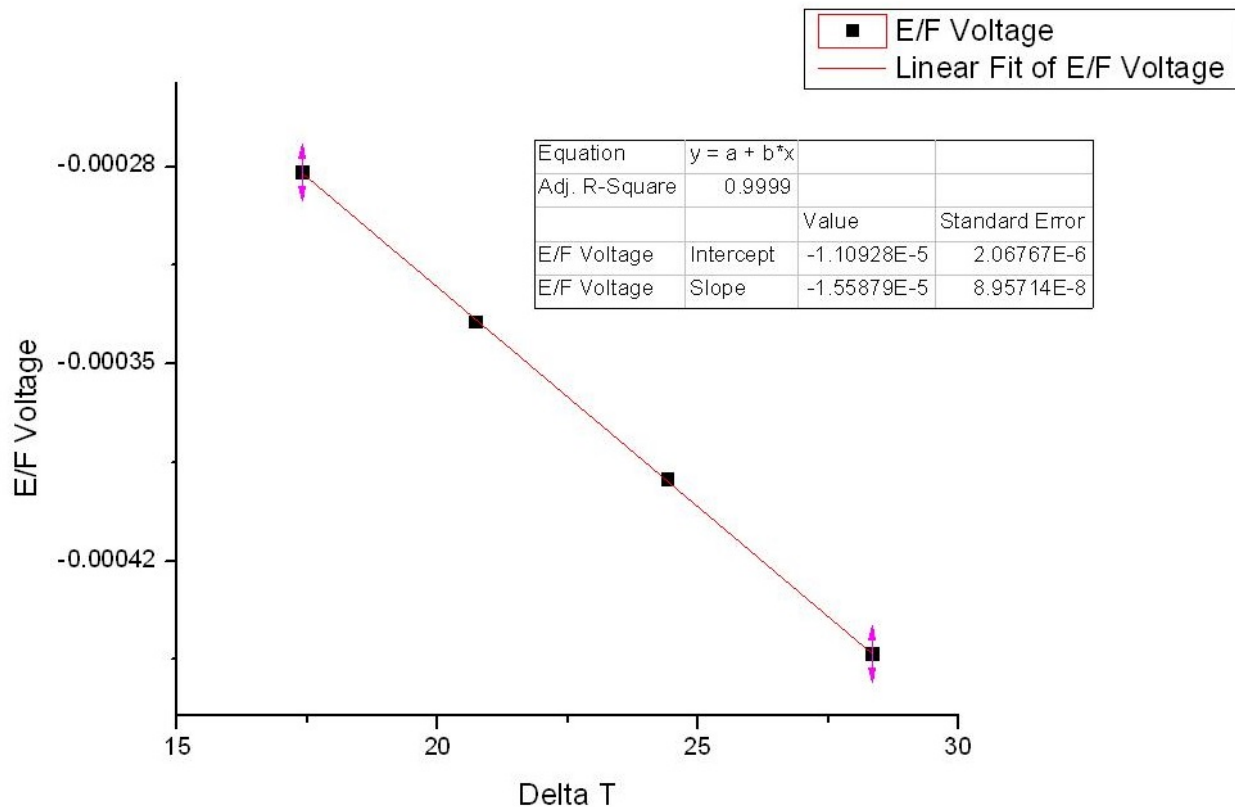
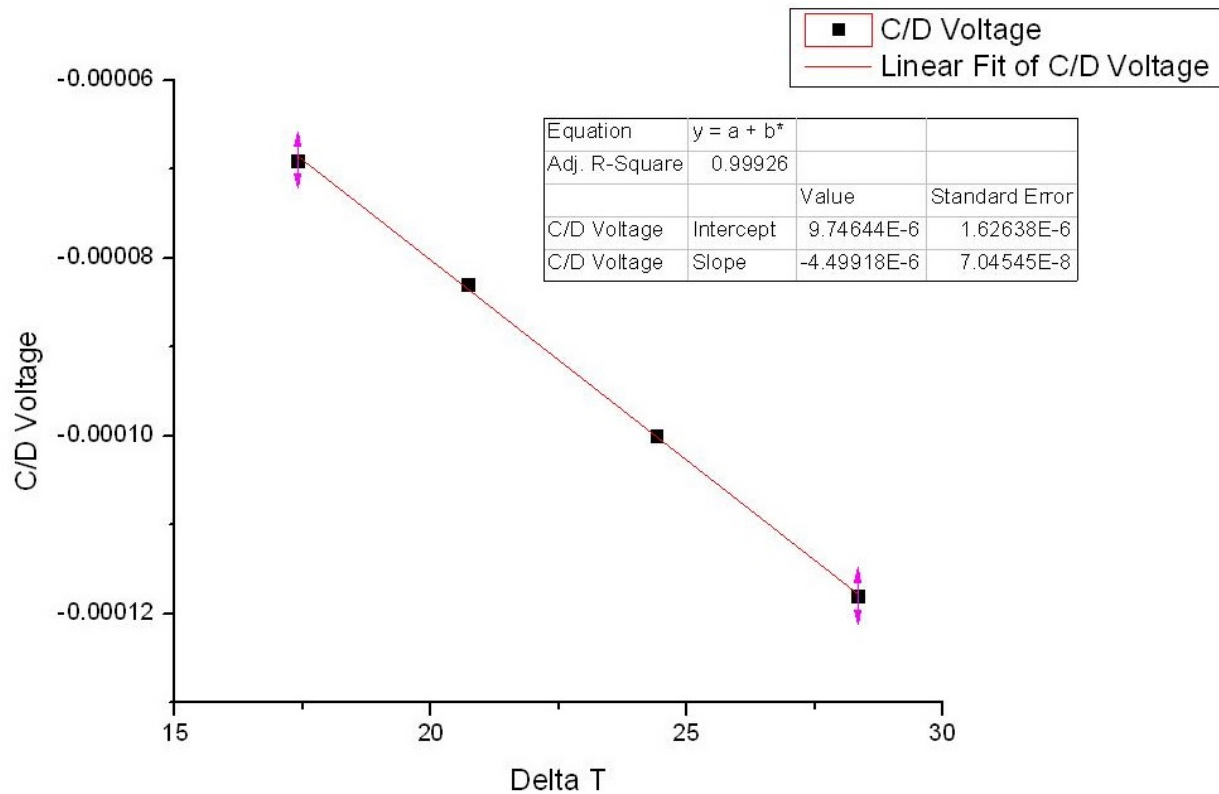


Figure 4.11. Plot of E/F Voltage vs.  $\Delta T$  for BiSbTe sample.



**Figure 4.12. Plot of C/D Voltage vs.  $\Delta T$  for BiSbTe sample.**

Using equation 3.9 and using the E/F Slope gives a Nernst coefficient of  $8.888 \times 10^{-9}$  V/(G·K), or  $8.888 \times 10^{-5}$  V/(T·K). Using the C/D Slope instead gives a Nernst coefficient of  $2.5655 \times 10^{-9}$  V/(G\*K), or  $2.5655 \times 10^{-5}$  V/(T\*K).

## Chapter 5. Discussion

### 5.1. Improvement of Results

It is necessary to compare the results obtained to known results in order to verify that our results are correct. Bel et. al. (Bel, 2004) lists a value of  $1 \mu\text{V}/(\text{K} \cdot \text{T})$ , that is,  $10^{-10}$  V/(K·G), as a large Nernst coefficient. This agrees with our results at constant temperature gradient, but our results at constant magnetic field are approximately one order of magnitude larger than this. We theorize that this is due to small misalignments in the voltage leads on the sample.

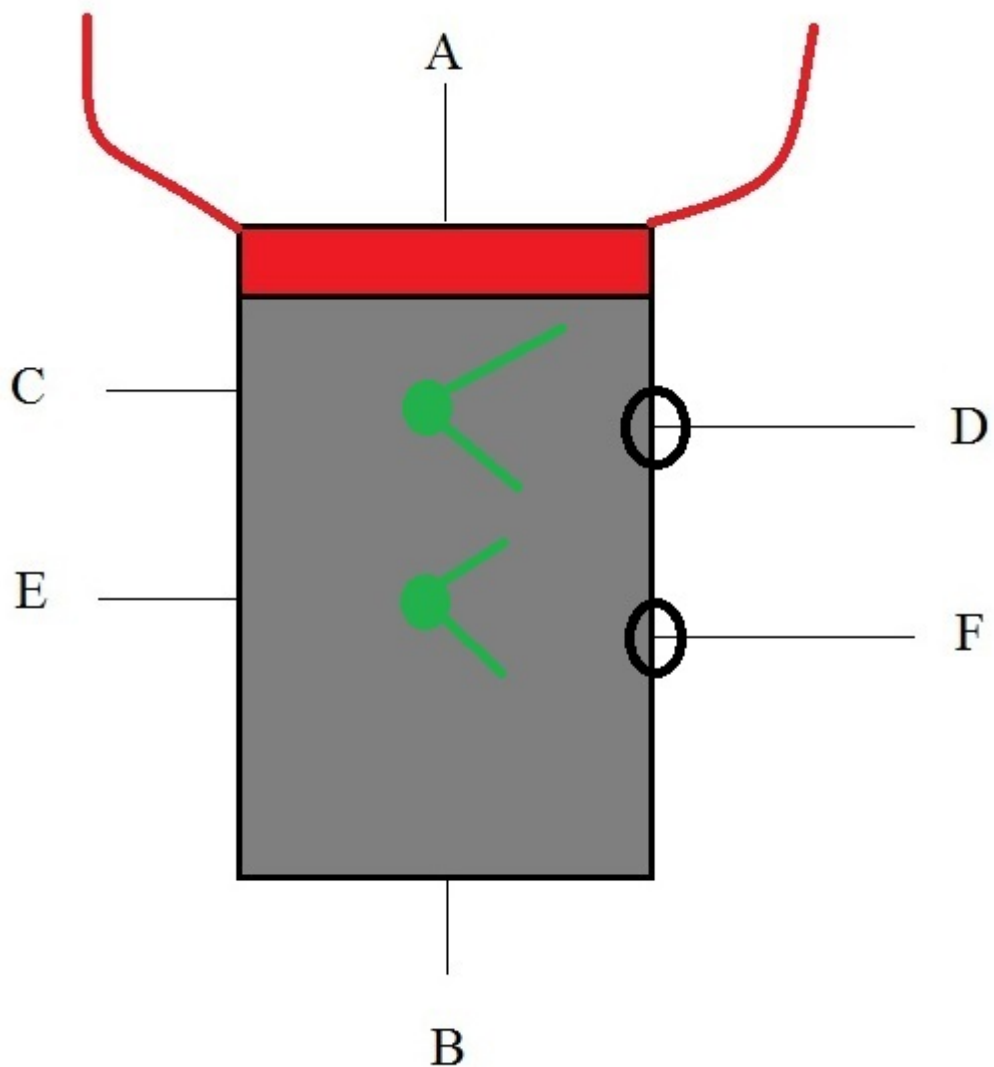


**Figure 5.1. Misalignment in the voltage leads on the sample.**

The misalignment causes a Seebeck voltage to develop when the temperature gradient is varied.

The Seebeck effect is a much stronger effect than the Nernst effect – as mentioned in Chapter 2,

the Seebeck coefficient is on the order of multiple  $\mu\text{V/K}$ , and  $1 \mu\text{V}/(\text{K}\cdot\text{T})$  is already a large

Nernst coefficient. Thus the voltage we read across the sample is larger than expected. This also

explains why the results at constant temperature gradient are as expected – since the temperature

is not being varied, there is no changing Seebeck voltage as we vary the magnetic field.

### 5.1.1. Error Analysis

In order to verify that the misalignment is the major source of error in our experimental setup, we took an error analysis of our experimental parameters using equation (3.5).

$$N = \frac{Vl}{dB\Delta T}$$

The total error of our experiment will be given by

$$\text{Total Error} = \sqrt{\left|\frac{\Delta V}{V}\right|^2 + \left|\frac{\Delta l}{l}\right|^2 + \left|\frac{\Delta d}{d}\right|^2 + \left|\frac{\Delta T}{T}\right|^2 + \left|\frac{\Delta B}{B}\right|^2} \quad (5.1)$$

Calculations for each term of equation 5.1 follow. Values for BiNiTe sample will be used. To calculate the error in the voltage, we will use the average E/F voltage values and take the average standard deviation for these values:

$$\left|\frac{\Delta V}{V}\right| = \frac{1.59723 \cdot 10^{-8}}{1.56823 \cdot 10^{-4}} = 1.0185 \cdot 10^{-4} \quad (5.2)$$

In calculating the error for  $l$ , the distance between the thermocouples, we measured the spot size of the BiNiTe sample to be 0.833 mm. We can determine the location of each wire to approximately half the spot size, or 0.4167 mm.

$$\left|\frac{\Delta l}{l}\right| = \frac{6.1278 - 5.2944}{5.7111} = 0.1459 \quad (5.3)$$

Error for  $d$ , the thickness of the sample, was calculated by taking a thickness measurement at both the top and the bottom of the sample. The sample is not perfectly rectangular and this will introduce a small error into the measurement.

$$\left|\frac{\Delta d}{d}\right| = \frac{2.48 - 2.44}{2.44} = 0.0164 \quad (5.4)$$

As previously mentioned in equations 3.2 and 3.3, we cannot directly calculate  $T$  at the thermocouples and we employ an approximation using the base sensitivity. These sensitivity

values are tabulated by NIST for type T thermocouples by listing values of thermocouple EMF for different temperature values. Values are listed from -270 °C to 400 °C. The following graph shows values at 20 °C.

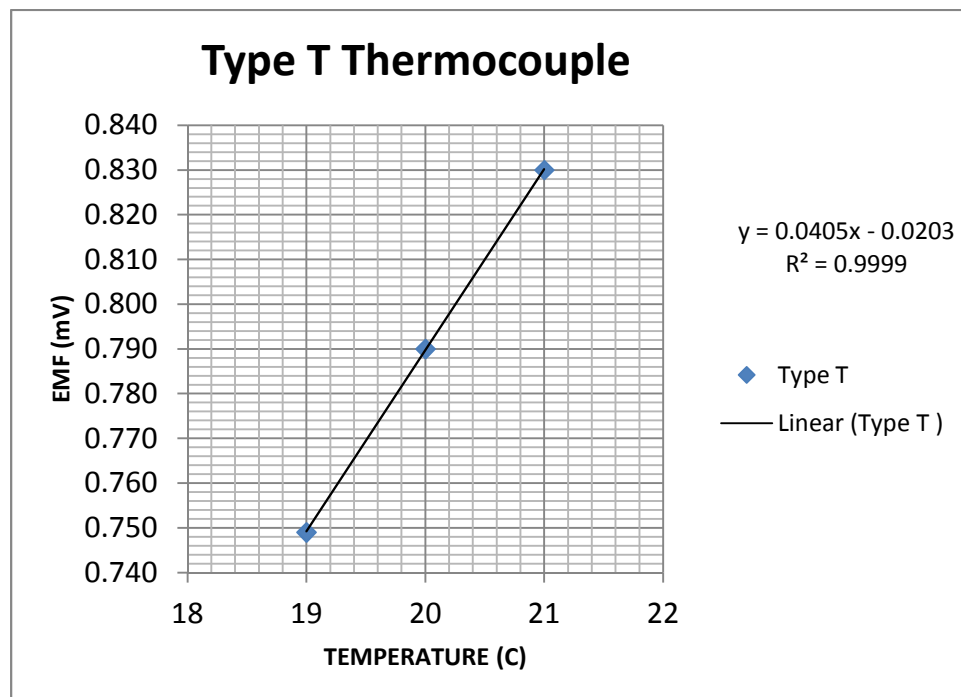


**Figure 5.2. Graph of Temperature vs. Thermocouple EMF. The sensitivity value at 20 °C is 0.0405 mV/°C.**

We calculated sensitivity values at given temperatures by linear fit of temperature vs. EMF values. The LabView program simply looks up the nearest sensitivity value for a given base temperature. The sensitivity values vary by approximately 6% over a 10 °C range, so the error in sensitivity measurements could be as large as 6%.

Magnetic field measurements are taken in 500 Gauss steps and are accurate within a tolerance of 1 Gauss.

$$\left| \frac{\Delta B}{B} \right| = \frac{1}{500} = 4 \cdot 10^{-6} (5.5)$$

Substituting the results from equations 5.2-5.5 and figure 5.2 into equation 5.1 gives a total error of 0.1586, or 15.86%. As expected, the thermocouple distance term is the majority of

the source of error in our measurements. 15% of the distance between the thermocouples is approximately half a millimeter. Assuming a temperature gradient of 3 K/mm, this results in a 1.5 K error. If we assume a Seebeck coefficient of 250  $\mu\text{V}/\text{K}$ , this error produces a voltage of up to 375  $\mu\text{V}$ , which is many orders of magnitude larger than the Nernst voltage.

The following table serves to summarize our error analysis.

Term	Error	% Error (Error · 100%)
V	$1.02 \cdot 10^{-4}$	$1.02 \cdot 10^{-2}\%$
l	0.15	15%
d	0.016	1.6%
T	0.06	6%
B	$4 \cdot 10^{-6}$	$4 \cdot 10^{-4}\%$

**Table 5.1. Summary of errors for terms in equation 3.5.**

### 5.1.2. *Improvements to Experimental Setup*

We first thought to use silver paste as an adhesive for the voltage leads rather than soldering the leads directly on the sample. Silver paste is an extremely conductive adhesive and is much easier to work with than solder, so aligning the leads would be much simpler for one to do. However, voltage readings with silver paste instead of solder were extremely poor and thus silver paste proved to not be a viable solution to the misalignment problem.

One solution proposed for the misalignment problem is the construction of a small, rotating sample holder. The holder would allow rotation of the sample in all three directions and would make it possible to precisely solder voltage leads onto the sample.

Another proposed solution is the use of a shadow mask. Using a shadow mask, we could sputter metal contacts directly onto the sample.

## **Chapter 6. Conclusions**

Our results show that the system we designed is capable of measuring the Nernst effect.

These results also showed that special care must be taken in aligning the voltage leads on the sample. Future work will involve solving the alignment problem. Additionally, the system as designed will also be able to take Hall Effect readings (using the 25 pin connector), Seebeck Effect readings, and electrical conductivity measurements.

## Bibliography

- R. Bel et al. *Giant Nernst Effect in CeCoIn<sub>5</sub>*. Physical Review Letters, Volume 92, Number 21. 2004.
- H. Julian Goldsmid. *Introduction to Thermoelectricity*. Springer-Verlag, 2010.
- E.H. Putley. *The Hall Effect and Related Phenomena*. Butterworth and Co. 1960.
- D.M. Rowe. *Thermoelectrics Handbook: Macro to Nano*. CRC Press, 2006.
- S.M. Sze and Kwok K. Ng. *Physics of Semiconductor Devices*. John Wiley and Sons, Inc. 2007.

## Vita

The author was born in Houston, Texas. He obtained his Bachelor of Science degree in Physics from Loyola University, New Orleans in 2011. He entered the University of New Orleans physics graduate program the same year to pursue a masters degree in applied physics and became a member of the Stokes research group.